Non-invasive Assessment of Mesenteric Hemodynamics in Patients with Suspected Chronic Mesenteric Ischemia using 4D flow MRI

Journal:	*Journal of Magnetic Resonance Imaging*
Manuscript ID	Draft
Wiley - Manuscript type:	Original Research
Classification:	Flow imaging < Imaging Principles and Education < Basic Science, Lower abdomen (kidneys, retroperitoneum, colon) < Body imaging < Clinical Science, MR angiography < Cardiovascular and interventional imaging < Clinical Science, Physiological research applications < Imaging Principles and Education < Basic Science, Functional body imaging < Body imaging < Clinical Science
Manuscript Keywords:	4D flow MRI, phase contrast, radial undersampling, atherosclerosis, chronic mesenteric ischemia, abdominal

Title:

Non-invasive Assessment of Mesenteric Hemodynamics in Patients with Suspected Chronic Mesenteric Ischemia using 4D flow MRI

Abstract:

Background:

Chronic mesenteric ischemia (CMI) is a rare disease with a particularly difficult diagnosis that results in inadequate blood flow to the small intestine, particularly after meals.

Purpose:

To quantitatively compare mesenteric hemodynamics before and after a standardized meal challenge in patients suspected of having CMI and individuals asymptomatic of CMI or vascular disease.

Study Type:

Retrospective.

Subjects:

Nineteen patients suspected of CMI and twenty control subjects.

Field Strength/Sequence:

Subjects were scanned at either 1.5T or 3.0T using a radially-undersampled 4D flow MR sequence (PC-VIPR) covering a large imaging volume with high spatial resolution.

Assessment:

Volumetric flow rates were assessed in the supraceliac (SCAo) and infrarenal (IRAo) aorta, celiac artery (CA), superior mesenteric artery (SMA), left and right renal arteries, superior mesenteric

vein (SMV), splenic vein, and portal vein (PV) in a fasting state (preprandial) and 20 minutes after a 700 kcal liquid meal (postprandial). Patients were subcategorized into positive diagnosis (CMI+, N=6) and negative diagnosis (CMI-, N=13) groups based on clinical findings.

Statistical Tests:

For each subject, preprandial and postprandial flow rates were compared using a paired t-test. These measures, as well as percent change in flow, were also compared between subgroups using a Welch t-test.

Results:

In controls and CMI- patients, SCAo, SMA, SMV, and PV flow increased significantly after meal ingestion. No significant flow increases were observed in CMI+ patients. Percent changes in SCAo, SMA, SMV, and PV flow were significantly greater in controls compared to CMI+ patients. Additionally, percent changes in flow in the SCAo, SMV, and PV were significantly greater in CMI- patients compared to CMI+ patients.

Data Conclusion:

4D flow MRI with large volumetric coverage demonstrated significant differences in the redistribution of blood flow in the SCAo, SMA, SMV, and PV in CMI+ patients after a meal challenge. This approach may assist in the challenging diagnosis of CMI.

Level of Evidence:

3

Technical Efficacy:

Stage 3

Keywords:

4D flow MRI; phase contrast; radial undersampling; hemodynamics; atherosclerosis; chronic mesenteric ischemia

Introduction:

Chronic mesenteric ischemia (CMI) is a diseased caused by underlying stenotic and occlusive diseases typically affecting the proximal portions of the primary mesenteric vessels – the celiac artery (CA), superior mesenteric artery (SMA), and inferior mesenteric artery (IMA) – resulting in inadequate blood flow to the small intestine following meal ingestion (1). While mesenteric artery stenoses are relatively common in aging populations, chronic mesenteric ischemia is rare because of collateral pathways within the mesenteric vasculature that often compensate for reduced blood flow (2). Thus, it is commonly recognized that at least 2 of the 3 main mesenteric arteries must be occluded to result in symptomatic CMI (3). In patients with CMI, the normal increase in mesenteric blood flow after meal consumption (postprandial hyperemia) is stunted causing dull, postprandial abdominal pain 15-60 minutes after meal ingestion with pain continuing up to 4 hours. This subsequently leads to fear of food, severe weight loss, malnutrition, and can eventually progress to acute-on-chronic mesenteric ischemia which is associated with a high mortality rate (4). Operative and endovascular interventions are treatment options that are often successful (5), but the proper diagnosis of CMI is difficult and requires a high index of clinical suspicion with currently no well-established diagnostic criteria.

If clinical findings strongly suggest CMI, contrast-enhanced CT angiography (CTA) of the abdomen is usually the first diagnostic exam of choice because it can identify and locate regions of stenosis and occlusion, as well as simultaneously exclude other abdominal pathologies (6,7). Contrast-enhanced magnetic resonance angiography (CE-MRA) may also be used, with studies demonstrating both high sensitivity and specificity in detecting proximal mesenteric lesions (8,9). However, CTA and CE-MRA lack functional information regarding mesenteric blood flow, the underlying physiological component of the disease. Duplex sonography has shown some success

in characterizing the extent of stenoses in patients suspected of CMI and has demonstrated that evaluating blood hemodynamics before and after a meal challenge can provide additional diagnostic information (10-12). However, sonography is not always feasible due to technical limitations, such as bowel gas overlying vessels of interest, excess adipose tissue, variable anatomy, and operator dependence (13).

Two-dimensional time-resolved phase-contrast magnetic resonance imaging (2D PC-MRI) has shown promise in non-invasively screening patients with suspected CMI by measuring volumetric blood flow rates in mesenteric vasculature to evaluate postprandial hemodynamic responses (14-17). Using 2D PC-MRI, it was first shown by Li et al. (14) that postprandial flow augmentation in the SMA was reduced proportionally to the severity of atherosclerosis in mesenteric vessels. A subsequent study by Burkart et al. (15) used 2D PC-MRI to prospectively evaluate suspected CMI patients by measuring volumetric blood flow rates in the superior mesenteric vein (SMV) before and after a meal; results showed a drastically impaired hemodynamic response in the SMV in patients with true CMI compared to those who were symptomatic but did not have CMI (as determined by angiography and clinical follow-up studies). A second study by Li et al. (16) reinforced these findings by showing that reduced postprandial flow augmentation occurs in both the SMV and SMA in patients with CMI. Despite these encouraging results, 2D PC-MRI is cumbersome in that it requires flow measurements in multiple vessel segments, which are patient-specific based on individual anatomy. Hence, an additional good-quality MR angiogram is required to identify the major vessels and potentially involved collaterals so that imaging planes can be placed perpendicular to vessel paths of interest. This leads to increased scan times and variability due to operator involvement.

Volumetric, time-resolved PC-MR with three-dimensional velocity encoding (4D flow MRI) has emerged as a compelling approach that can simultaneously interrogate large vascular territories for 3D MRA and functionally assess mesenteric hemodynamics all in one scan session (18). Due to the volumetric nature of the acquisition, any vessel within the 3D field of view can be retrospectively analyzed without additional scan time penalty. A recent study using 4D flow demonstrated the feasibility of a meal challenge in evaluating hepatic and mesenteric blood flow responses in portal hypertension patients (19). In this work, we use a similar 4D flow MRI approach to quantify the effects of a meal challenge in patients suspected of CMI and in healthy control subjects, thereby taking advantage of the large volumetric coverage to comprehensively assess the flow response in multiple mesenteric vascular segments.

Materials and Methods:

Subjects

In this Health Insurance Portability and Accountability Act (HIPAA)-compliant and Institutional Review Board (IRB)-approved retrospective study, 21 consecutive patients (15 females, mean age: 47.5 years [21-86], mean weight: 69.2 kg) with a suspicion of CMI were scanned according to our clinical CMI protocol. Studies were performed between March 2012 and August 2019 on patients referred from vascular surgery or gastroenterology based on a clinical presentation typical of CMI. Of the 21 patients, 4D flow data were successfully obtained in 19 patients (14 females, mean age: 50.1 years [21-86], mean weight: 68.8 kg). Two cases could not be analyzed due to high levels of noise resultant from acquisition errors and were excluded from the study. Patients were subcategorized into positive (CMI+) and negative (CMI-) groups based on imaging and clinical findings. Patients were deemed CMI+ if MRA imaging indicated 2 or more primary vessel occlusions of grade 2 or higher (8) and if clinical findings strongly suggested CMI (2). Image

interpretation and clinical diagnoses were performed by a trained cardiovascular radiologist (XXX) with 17 years of experience. Twenty control subjects (8 females, mean age: 44.4 years [19-73], mean weight: 80.2 kg) underwent the same CMI protocol as the patient cohort and were analyzed retrospectively. Control subjects were defined as individuals asymptomatic of CMI or other vascular disease.

Imaging Protocol

Control subjects were scanned on a clinical 3.0T scanner (Discovery MR750, GE Healthcare, Waukesha, WI) with a 32-channel phase-array torso coil (NeoCoil, Pewaukee, WI). Subjects from the CMI+ and CMI- groups were scanned on either a clinical 1.5T or 3.0T scanner (Signa HDX, Optima 540w, or Discovery MR750, GE Healthcare, Waukesha, WI) with various torso coils (8-channel, 12-channel, 24-channel, and 32-channel) based on scanner and coil availability at the time of examination. As part of the CMI protocol, 4D flow MRI was performed both before and after a standardized meal challenge. An initial preprandial scan was performed after at least 5 hours of fasting. Subsequently, subjects ingested 474 mL of Ensure Plus (700 kcal, 56% carbohydrates, 29% fats, 15% protein; Abbott Laboratories, Columbus, OH) followed by a second postprandial scan 20 minutes after meal ingestion. Twenty minutes was chosen to allow for sufficient arterial and venous blood flow responses to be observed (19,20).

4D flow MRI was performed using a 5-point, radially-undersampled acquisition (Phase Contrast Vastly undersampled Isotropic Projection Reconstruction, PC-VIPR) that provides high spatial resolution, increased motion robustness, and retrospective gating flexibility within a reasonable scan time (21,22). Complete volumetric coverage of the abdomen was acquired, centered over the celiac axis with the following imaging parameters: TR=6.6-8.3 ms; TE=1.9-2.7 ms; tip angle=14˚; number of projections=11,000; acquired isotropic resolution=1.25 mm; reconstructed imaging

volume=32 cm^3; scan time=11 minutes. Intravenous contrast agents containing 0.03 mmol/kg of gadofosveset trisodium (Lantheus, North Billerica, MA) were administered immediately before the preprandial scan in 17 controls and 19 patients. Three control subjects and one patient did not receive contrast agents due to contraindications or refusal. The velocity encoding (V_{enc}) was set to 100 cm/s for the preprandial scan and was increased to 120 cm/s for the postprandial scan to account for anticipated increases in mesenteric blood velocities. During image acquisition, ECG and respiratory monitoring were performed to allow for retrospective cardiac and respiratory gating during reconstruction.

Data Analysis and Flow Measurements

Reconstruction was performed offline yielding time-resolved and time-averaged magnitude, complex difference, and 3-directional velocity data. All time-resolved data were reconstructed into 14 cardiac timeframes using temporal view sharing (23). Background phase correction was performed on all datasets by fitting a 3rd order polynomial to phase in stationary tissue, defined by semi-automatically thresholding time-averaged magnitude and velocity data (24). Time-averaged complex difference data were exported to Mimics (Materialize, Leuven, Belgium) for semi-automatic vessel segmentation (global thresholding plus region growing) in order to create 3D angiogram masks, shown in Figure 1.

Angiograms and time-resolved velocity data were exported to Ensight (ANSYS, Canonsburg, PA) for visualization of blood flow patterns and interactive 2D plane placement for flow analysis. Color-coded vector streamline images and particle traces were created in Ensight to visualize time-resolved flow patterns (Figure 2). 2D cut-planes were manually placed in vessels of interest perpendicular to the direction of the vessel for quantitative flow analysis. Flow analysis was performed in 6 arteries: superior mesenteric artery (SMA), celiac artery (CA), supraceliac aorta

(SCAo), infrarenal aorta (IRAo), right renal artery (RRA), left renal artery (LRA), as well as 3 veins: superior mesenteric vein (SMV), splenic vein (SV), and portal vein (PV). All cut-planes were placed at least 3 diameters away from either a confluence or bifurcation to avoid regions of highly disturbed flow due to entrance effects. In some datasets, certain vessel segments could not be well visualized on the PC angiogram due to either an insufficient size of the imaging volume, vessel occlusions, or very slow flows. In these cases, flow analysis was not performed.

Data from the 2D cut-planes were exported to a customized software package (25) where manual, time-resolved segmentation was performed on all vessels (Figure 2a inset) to account for pulsatile vessel motion during the cardiac cycle. All planes were visually inspected to ensure that velocity aliasing had not occurred. Average volumetric flow rates were calculated by finding the mean volumetric flow rate over the cardiac cycle and normalizing that value by the subject's body weight (kg) to avoid influence of body size on flow rate magnitudes as has been done in similar studies (15-17,26-28). Percent changes in blood flow were calculated by subtracting average postprandial flow rates from average preprandial flow rates and dividing by the average preprandial flow rate. For each subject, average pre- and postprandial volumetric flow rates, as well as the percent change in flow values, were calculated for all visualized vessels. Group-averaged preprandial, postprandial, and percent change in flow values were calculated for all vessels by averaging values over all subjects in each of the three subgroups.

Internal Consistency Measurements

Internal consistency of flow measurements was assessed using conservation of flow in the measured arterial and venous segments. Conservation of flow would require the difference between SCAo and IRAo flow ($\overline{Q}_{loss}$) to be approximately equal to the sum of the flow of vessels

exiting between these two arterial segments ($\overline{Q}_{branch}$), as visualized in Figure 2a and represented in Eq. (1):

$$\overline{Q}_{loss} = \overline{Q}_{SCAo} - \overline{Q}_{IRAo} \approx \overline{Q}_{CA} + \overline{Q}_{SMA} + \overline{Q}_{RRA} + \overline{Q}_{LRA} = \overline{Q}_{branch} \#(1)$$

An analogous conservation law holds for venous flow measurements:

$$\overline{Q}_{PV} \approx \overline{Q}_{SV} + \overline{Q}_{SMV} \#(2)$$

As a means of comprehensively assessing internal consistency of flow, correlation analysis was used to compare measured arterial loss ($\overline{Q}_{loss}$) to measured flow from branching mesenteric arteries ($\overline{Q}_{branch}$) and similarly for flow in the portal vein ($\overline{Q}_{PV}$) and the sum of flow in the splenic and superior mesenteric veins ($\overline{Q}_{SV} + \overline{Q}_{SMV}$). Datasets with missing vessel segments (e.g. due to vessel location outside imaging volume, occlusions, or imaging artifacts) were excluded from this analysis.

Statistical Analysis

Within each subgroup, flow rate differences before and after a meal were compared using a two-tailed paired t-test. Additionally, preprandial, postprandial, and percent change in flow values were compared between subgroups using a two-tailed Welch t-test. For all statistical tests, $p<0.05$ was chosen to reflect statistical significance. Cohen's d effect sizes (29) were reported in conjunction with p-values.

For flow consistency analysis, all complete preprandial and postprandial datasets from each subgroup were combined and coefficients of determination (R^2 values) were obtained for arterial and venous measurements.

Results:

Flow analysis

After subject categorization, the cohorts consisted of 13 CMI- patients (7 females, mean age: 44.3 years [21-86], mean weight: 70.1 kg) in which findings did not support the diagnosis of CMI and 6 CMI+ patients (4 females, mean age: 62.5 years [42-80], mean weight: 64.2 kg), in which findings strongly suggested CMI. In some subjects, vessels were not visualized. Between all 78 preprandial and postprandial datasets, this occurred 2 times in the SCAo, 5 times in the IRAo, 2 times in the LRA, 6 times in the RRA, 4 times in the CA, 2 times in the SMV, 5 times in the SV, and 2 times in the PV, leaving 59 arterial and 69 venous datasets for consistency analysis. The SMA was visualized on all image sets. Average weight-corrected pre- and postprandial volumetric flow rates for each group are shown in Table 1-2. Average percent changes in flow for each group are given in Table 3 and visualized in Figure 3.

SCAo

In control subjects, SCAo blood flow increased significantly 20 minutes after a meal ($p=5.62e-05$, Cohen's $d=0.381$) as did blood flow in the CMI- group ($p=0.005$, $d=0.507$). In contrast, the CMI+ group showed no significant increase in blood flow after the meal ($p=0.592$, $d=0.107$). Postprandial SCAo flow rates for the CMI+ group were significantly lower than both the control group ($p=0.013$, $d=0.875$) and the CMI- group ($p=0.033$, $d=0.825$) while preprandial flow rates were not significantly different between subgroups. Percent change in SCAo flow for the CMI+ group was significantly less than both the CMI- group ($p=0.008$, $d=1.15$) and the control group ($p=0.022$, $d=0.956$). However, there was no significant difference in percent change in flow between controls and the CMI- group.

LRA and RRA

While not statistically significant, the CMI+ group trended towards decreased LRA percent change in flow values relative to the control group (p=0.080, d=0.774) and to the CMI- group (p=0.108, d=0.654). Similarly, percent change in RRA flow for the CMI+ group trended towards decreased values relative to the control group (p=0.060, d=1.04) and to the CMI- group (p=0.146, d=0.466) but was not found to be statistically significant.

SMA

While SMA blood flow increased significantly after a meal for control subjects (p=5.20e-06, d=1.26) and for the CMI- group (p=0.016, d=0.491), the CMI+ group did not see a significant increase (p=0.193, d=0.465). Percent change in SMA flow was significantly less in the CMI+ group compared to the control group (p=0.003, d=0.865) but was not significantly less compared to the CMI- group (p=0.104, d=0.529). Additionally, percent change in flow for the CMI- group was not significantly different from control subjects.

CA

CA blood flow did not increase significantly after a meal for any group, however, preprandial CA flow in the CMI- group was significantly higher than the control group (p=0.023, d=0.581). Preprandial CA flow in the CMI+ group was not significantly different from controls (p=0.096, d=0.468).

SMV

SMV blood flow increased significantly after a meal in the control group (p=2.51e-08, d=2.10) and in the CMI- group (p=3.05e-06, d=1.67). The CMI+ group did not see any significant increase in SMV flow after a meal (p=0.120, d=0.777). For the CMI+ group, preprandial SMV flow was significantly higher than the control group (p=0.040, d=0.905) but was not significantly higher

than the CMI- group (p=0.074, d=0.665). There was no significant difference in preprandial flow between the control group and the CMI- group. There were also no significant differences in postprandial SMV flow between any of the groups. Percent change in flow for the CMI+ group was significantly less compared to the control group (p=0.008, d=0.944) and the CMI- group (p=0.009, d=0.875).

PV

In control subjects, PV blood flow increased significantly after a meal (p=1.17e-05, d=1.137) as did the CMI- group (p=1.60e-05, d=1.690) while the CMI+ group did not see a significant increase in PV blood flow after a meal (p=0.243, d=0.362). Additionally, percent change in flow for the CMI+ group was significantly less than the control group (p=0.018, d=0.788) and the CMI- group (p=0.006, d=1.02).

Flow Consistency

Correlation analysis was successfully performed on all measured $\overline{Q}_{loss}$ and $\overline{Q}_{branch}$ values, as shown in Figure 4a. A strong correlation was found between $\overline{Q}_{loss}$ and $\overline{Q}_{branch}$ values (R^2=0.859). As seen in Figure 4a, postprandial $\overline{Q}_{loss}$ and $\overline{Q}_{branch}$ values were increased compared to preprandial $\overline{Q}_{loss}$ and preprandial $\overline{Q}_{branch}$ values. This result coincides with observed increases in mesenteric blood flow after a meal. Correlation analysis was also performed on all measured $\overline{Q}_{PV}$ and $(\overline{Q}_{SV} + \overline{Q}_{SMV})$ values, as shown in Figure 4b. A strong correlation between $\overline{Q}_{PV}$ and $(\overline{Q}_{SV} + \overline{Q}_{SMV})$ values was also observed (R^2=0.894). Furthermore, measured volumetric flow rates in this study agreed well with flow rates reported from other imaging modalities (14-17,19,26-28,30-36). 4D flow rates tended to be closer to those obtained by ultrasound and were consistently higher than those obtained using 2D PC-MRI.

PC Angiograms

PC angiograms were obtained for all 78 pre- and postprandial cases. Locations of likely occlusions, as well as collateral mesenteric vessels, were observed in a variety of patients. Figure 5a shows an example of a patient with median arcuate ligament syndrome in which the median arcuate ligament was compressing the CA. Despite this obstruction, flow in the splenic artery and gastroduodenal artery (GDA) was preserved due to a portion of SMA blood flow being redirected back through the pancreaticoduodenal arcades. The CA could not be visualized on the PC angiogram in this patient. Fasting flow in the GDA was approximately 24.3% of the measured fasting flow in the SMA, which decreased to 7.4% after a meal. However, flow in the SMA and SMV increased to a normal range following a meal (104% and 236% respectively).

Figure 5b shows a CMI+ patient with a full SMA occlusion (as seen in the PC angiogram) and celiac artery with narrowing. Flow was redirected from the CA to the SMA (just distal to the occlusion) via the pancreaticoduodenal arcades, which were well-visualized on the PC angiogram. Distal SMA flow decreased by 7.13% following a meal and SMV flow increased only slightly by 2.93%. Additionally, supplementary collateral flow from the IMA (via Arc of Riolan) was prominent in the angiogram.

Discussion:

In this study, 4D flow MRI was used to obtain comprehensive hemodynamic measurements of the mesenteric vasculature in patients suspected of chronic mesenteric ischemia (CMI) and in control subjects both before and after meal ingestion. Our results were consistent with previous 2D PC-MRI imaging studies (14-17) and demonstrated the potential of 4D flow MRI studies to help disentangle the complex flow patterns observed in CMI. Firstly, 4D flow MRI provides simultaneous acquisition of both hemodynamic information and an MRA. Previous studies showed

that 3D PC MRA can accurately measure vessel lumens of renal arteries (37) and identify areas of stenoses in suspected chronic mesenteric patients (38). Secondly, the large volumetric coverage ensures all relevant vessels and collaterals are visualized without the need for a dedicated MRA that often requires injection of a contrast agent. This may be useful since many patients demonstrate significant anatomical variations and may help overcome user- and patient-dependent issues associated with ultrasound. Thirdly, retrospective analysis is possible for any vessel (including collaterals) within the imaging volume without scan time penalty, unlike 2D PC-MRI. Lastly, 4D flow MRI using an accelerated sequence such as PC-VIPR requires only a short 10-minute free-breathing scan session while retaining high temporal and spatial resolution.

Flow Consistency

Correlation analysis showed strong correlation between $\overline{Q}_{loss}$ (the difference between SCAo and IRAo flow rates) and $\overline{Q}_{branch}$ (sum of flow rates in vessels exiting between these aortic segments) in both the arterial measurements and venous segments ($\overline{Q}_{PV}$ and $\overline{Q}_{SV} + \overline{Q}_{SMV}$). The slope for both regression models was less than unity, indicating that some flow was not being accounted for in the $\overline{Q}_{branch}$ and $\overline{Q}_{SV} + \overline{Q}_{SMV}$ measurements. This discrepancy is likely due to small, unmeasured collaterals and measurement errors. Despite this, the strong correlation reflects good internal consistency and thus supports the feasibility of 4D flow measurements. Additionally, flow rates in this study agreed well with flow rates reported from other imaging modalities.

Flow Analysis

Both the control subjects and symptomatic patients without CMI (CMI-) experienced significant blood flow increases in the SMA, SMV, and PV twenty minutes after meal ingestion. This is expected in normal individuals because an increase in SMA flow is needed to satisfy the increased metabolic demands of the gastrointestinal tract (20,32). Since a majority of arterial mesenteric

flow is returned through the SMV, increases in arterial flow will lead to increases in venous flow in the SMV and subsequently PV, which was observed in this study. Furthermore, an increase in SCAo blood flow was observed in controls and in the CMI- group. This is most likely due to increased cardiac output following meal ingestion, acting to increase volumetric flow rates in the aorta (39). On the other hand, symptomatic patients with true CMI (CMI+ group) experienced no significant postprandial blood flow increases in any vessel. Furthermore, postprandial blood flow responses (percent changes in blood flow) in the SMA, SMV, and PV were significantly decreased in CMI+ patients compared to controls, supporting findings from prior 2D PC-MRI studies (14-17). Postprandial blood flow responses in the SCAo were also decreased in CMI patients compared to controls which has not been previously shown. Postprandial blood flow increases in the CA were not observed for any group. Since the CA primarily supplies proximal portions of the gastrointestinal tract, blood flow responses occur almost immediately after a meal and return to baseline levels shortly thereafter (20). In this study, patients were imaged 20 minutes after ingestion of a meal, allowing postprandial CA flow rates to return to near baseline levels, explaining the negligible observed increases in CA flow rates.

In addition, postprandial blood flow responses for the CMI+ group were significantly decreased in the SCAo, SMV, and PV, compared to the CMI- group, while SMA flow responses were not. SMA flow responses in the CMI- group may be lower due to several patients with narrowing celiac arteries. In these patients, preprandial SMA flow values tended to be higher than in control subjects, which has also been observed in other studies (16,17). We theorize that, due to blood flow restriction in the CA, flow that would have otherwise entered the CA is being directed to the SMA, resulting in higher preprandial flow values and thus diminished SMA flow responses. It should also be noted that, in these patients, SMV and PV flow still increased to normal levels.

It was also observed that SMV preprandial flow rates were increased in CMI+ patients compared to controls. The explanation for this relationship is not readily apparent. However, similar results were seen in other studies (16,17) in which average fasting SMV flow rates were slightly higher in diseased patients.

Limitations

Due to the nature of this retrospective study, scans were acquired with 1.5T and 3.0T scanners and with slightly varying imaging protocols. While this might affect image quality, it should have very minor implications on the flow measurements used here. Additionally, classifying patients as ischemic versus non-ischemic based on MRA stenoses measurements and clinical findings may be prone to error due to the lack of a widely-accepted gold standard imaging method. The post-processing workflow required some manual processing steps such as vessel segmentation and analysis plane placement, decreasing repeatability and increasing the time required to process cases. This problem could be alleviated by developing an automated pipeline for image segmentation and flow analysis. Lastly, a larger patient sample size, particularly a larger CMI+ group, is warranted to further verify the findings in this study.

Future Directions

Flow measurements in all 3 main mesenteric arteries (CA, SMA, and IMA) would provide a more comprehensive analysis of arterial inflow to the small intestine. Because we aimed to measure flow in the SCAo, the IMA was often out of frame even despite the large imaging volume provided by the PC-VIPR sequence used in this study. Flow measurements in this vessel would be particularly valuable in assessing patients with CA and SMA lesions, as the IMA may contribute a large portion of flow via collaterals, such as the Arc of Riolan and the marginal artery of Drummond. Further classification of patients based on stenoses location and severity obtained

from either MRA or PC MRA angiograms may also be warranted to provide more insight into distinct hemodynamic flow patterns in the mesenteric vessels and associated collaterals. Additional information may also be gained by investigating the temporal evolution of blood flow patterns in the primary mesenteric vessels (CA, SMA, and IMA) and collaterals using 4D flow MRI. It has been theorized (40) that gastric hyperemia shortly after meal ingestion causes shunting of blood from the SMA, which may be responsible for the sudden onset of pain (well before food has reached the small intestine) in CMI patients with poor splanchnic blood flow reserve. As noted previously, increases in CA blood flow (gastric hyperemia) occur very soon after meal ingestion (20). Acquiring multiple 4D flow MRI scans where blood flow changes are measured in the CA, SMA, IMA, and associated collaterals at different points in the digestion phase may provide further insight into the temporal nature of blood flow patterns and the hemodynamic basis for postprandial pain. Accelerated 4D flow MRI approaches such as PC-VIPR are well-suited for this type of investigation because of short scan times, allowing for multiple vessels to be retrospectively analyzed at various points along the digestion phase.

Conclusion

In conclusion, 4D flow MRI is a promising non-invasive diagnostic technique that can functionally and anatomically evaluate mesenteric vasculature. 4D flow MRI possesses the unique capability of obtaining complete volumetric hemodynamic information in a single scan, allowing for the quantitative assessment of blood flow patterns in multiple mesenteric vessels, while also producing a high-quality PC angiogram to morphologically assess stenoses and occlusions. The blood flow measurements obtained in this study showed good internal consistency and flow measures results were comparable to prior 2D PC-MRI and ultrasound studies measuring mesenteric blood flow. Here, we found quantifiable differences in blood flow hemodynamics in the aorta, SMA, SMV,

and PV between individuals diagnosed with CMI, those who were symptomatic but did not have CMI, and control subjects. Additional studies with larger patient cohorts are needed to investigate whether 4D flow MRI can improve the accuracy in the challenging diagnosis of mesenteric ischemia and thereby improve treatment planning and patient care.

References:

1. van Bockel JH, Geelkerken RH, Wasser MN. Chronic splanchnic ischaemia. Best Pract Res Clin Gastroenterol 2001;15(1):99-119.
2. Kolkman JJ, Geelkerken RH. Diagnosis and treatment of chronic mesenteric ischemia: An update. Best Pract Res Clin Gastroenterol 2017;31(1):49-57.
3. Stanton PE, Hollier PA, Seidel TW, Rosenthal D, Clark M, Lamis PA. Chronic intestinal ischemia: Diagnosis and therapy. Journal of Vascular Surgery 1986;4(4):338-344.
4. Sreenarasimhaiah J. Chronic mesenteric ischemia. Best Pract Res Clin Gastroenterol 2005;19(2):283-295.
5. Pillai AK, Kalva SP, Hsu SL, et al. Quality Improvement Guidelines for Mesenteric Angioplasty and Stent Placement for the Treatment of Chronic Mesenteric Ischemia. J Vasc Interv Radiol 2018;29(5):642-647.
6. Oliva IB, Davarpanah AH, Rybicki FJ, et al. ACR Appropriateness Criteria (R) imaging of mesenteric ischemia. Abdom Imaging 2013;38(4):714-719.
7. Amin MA, Nooman NA, Moussa GI. Acute and chronic mesenteric ischemia: Multidetector CT and CT angiographic findings. The Egyptian Journal of Radiology and Nuclear Medicine 2014;45(4):1063-1070.
8. Carlos RC, Stanley JC, Stafford-Johnson D, Prince MR. Interobserver variability in the evaluation of chronic mesenteric ischemia with gadolinium-enhanced MR angiography. Acad Radiol 2001;8(9):879-887.
9. Meaney JF, Prince MR, Nostrant TT, Stanley JC. Gadolinium-enhanced MR angiography of visceral arteries in patients with suspected chronic mesenteric ischemia. J Magn Reson Imaging 1997;7(1):171-176.

10. Zwolak RM, Fillinger MF, Walsh DB, et al. Mesenteric and celiac duplex scanning: a validation study. J Vasc Surg 1998;27(6):1078-1087; discussion 1088.

11. Muller AF. Role of duplex Doppler ultrasound in the assessment of patients with postprandial abdominal pain. Gut 1992;33(4):460-465.

12. Gentile AT, Moneta GL, Lee RW, Masser PA, Taylor LM, Jr., Porter JM. Usefulness of fasting and postprandial duplex ultrasound examinations for predicting high-grade superior mesenteric artery stenosis. Am J Surg 1995;169(5):476-479.

13. Sabba C, Ferraioli G, Sarin SK, Lerner E, Groszmann RJ, Taylor KJ. Feasibility spectrum for Doppler flowmetry of splanchnic vessels. In normal and cirrhotic populations. J Ultrasound Med 1990;9(12):705-710.

14. Li KC, Whitney WS, McDonnell CH, et al. Chronic mesenteric ischemia: evaluation with phase-contrast cine MR imaging. Radiology 1994;190(1):175-179.

15. Burkart DJ, Johnson CD, Reading CC, Ehman RL. MR measurements of mesenteric venous flow: prospective evaluation in healthy volunteers and patients with suspected chronic mesenteric ischemia. Radiology 1995;194(3):801-806.

16. Li KC, Hopkins KL, Dalman RL, Song CK. Simultaneous measurement of flow in the superior mesenteric vein and artery with cine phase-contrast MR imaging: value in diagnosis of chronic mesenteric ischemia. Work in progress. Radiology 1995;194(2):327-330.

17. Dalman RL, Li KC, Moon WK, Chen I, Zarins CK. Diminished postprandial hyperemia in patients with aortic and mesenteric arterial occlusive disease. Quantification by magnetic resonance flow imaging. Circulation 1996;94(9 Suppl):Ii206-210.

18. Roldan-Alzate A, Francois CJ, Wieben O, Reeder SB. Emerging Applications of Abdominal 4D Flow MRI. AJR Am J Roentgenol 2016;207(1):58-66.

19. Roldan-Alzate A, Frydrychowicz A, Said A, et al. Impaired regulation of portal venous flow in response to a meal challenge as quantified by 4D flow MRI. J Magn Reson Imaging 2015;42(4):1009-1017.

20. Someya N, Endo MY, Fukuba Y, Hayashi N. Blood flow responses in celiac and superior mesenteric arteries in the initial phase of digestion. Am J Physiol Regul Integr Comp Physiol 2008;294(6):R1790-1796.

21. Gu T, Korosec FR, Block WF, et al. PC VIPR: a high-speed 3D phase-contrast method for flow quantification and high-resolution angiography. AJNR Am J Neuroradiol 2005;26(4):743-749.

22. Johnson KM, Markl M. Improved SNR in phase contrast velocimetry with five-point balanced flow encoding. Magn Reson Med 2010;63(2):349-355.

23. Liu J, Redmond MJ, Brodsky EK, et al. Generation and visualization of four-dimensional MR angiography data using an undersampled 3-D projection trajectory. IEEE Trans Med Imaging 2006;25(2):148-157.

24. Walker PG, Cranney GB, Scheidegger MB, Waseleski G, Pohost GM, Yoganathan AP. Semiautomated method for noise reduction and background phase error correction in MR phase velocity data. J Magn Reson Imaging 1993;3(3):521-530.

25. Stalder AF, Russe MF, Frydrychowicz A, Bock J, Hennig J, Markl M. Quantitative 2D and 3D phase contrast MRI: optimized analysis of blood flow and vessel wall parameters. Magn Reson Med 2008;60(5):1218-1231.

26. Burkart DJ, Johnson CD, Ehman RL. Correlation of arterial and venous blood flow in the mesenteric system based on MR findings. 1993 ARRS Executive Council Award. AJR Am J Roentgenol 1993;161(6):1279-1282.

27. Burkart DJ, Johnson CD, Morton MJ, Wolf RL, Ehman RL. Volumetric flow rates in the portal venous system: measurement with cine phase-contrast MR imaging. AJR Am J Roentgenol 1993;160(5):1113-1118.

28. Moriyasu F, Ban N, Nishida O, et al. Clinical application of an ultrasonic duplex system in the quantitative measurement of portal blood flow. J Clin Ultrasound 1986;14(8):579-588.

29. Cohen J. Statistical power analysis for the behavioral sciences. Hillsdale, N.J.: L. Erlbaum Associates: 1988.

30. Les AS, Yeung JJ, Schultz GM, Herfkens RJ, Dalman RL, Taylor CA. Supraceliac and Infrarenal Aortic Flow in Patients with Abdominal Aortic Aneurysms: Mean Flows, Waveforms, and Allometric Scaling Relationships. Cardiovasc Eng Technol 2010;1(1).

31. Taylor CA, Cheng CP, Espinosa LA, Tang BT, Parker D, Herfkens RJ. In vivo quantification of blood flow and wall shear stress in the human abdominal aorta during lower limb exercise. Ann Biomed Eng 2002;30(3):402-408.

32. Sieber C, Beglinger C, Jaeger K, Hildebrand P, Stalder GA. Regulation of postprandial mesenteric blood flow in humans: evidence for a cholinergic nervous reflex. Gut 1991;32(4):361-366.

33. Moneta GL, Taylor DC, Helton WS, Mulholland MW, Strandness DE, Jr. Duplex ultrasound measurement of postprandial intestinal blood flow: effect of meal composition. Gastroenterology 1988;95(5):1294-1301.

34. Cooper AM, Braatvedt GD, Qamar MI, et al. Fasting and post-prandial splanchnic blood flow is reduced by a somatostatin analogue (octreotide) in man. Clin Sci (Lond) 1991;81(2):169-175.

35. Nishida O, Moriyasu F, Nakamura T, et al. Interrelationship between splenic and superior mesenteric venous circulation manifested by transient splenic arterial occlusion using a balloon catheter. Hepatology 1987;7(3):442-446.

36. Gaiani S, Bolondi L, Bassi SL, Santi V, Zironi G, Barbara L. Effect of meal on portal hemodynamics in healthy humans and in patients with chronic liver disease. Hepatology 1989;9(6):815-819.

37. Francois CJ, Lum DP, Johnson KM, et al. Renal arteries: isotropic, high-spatial-resolution, unenhanced MR angiography with three-dimensional radial phase contrast. Radiology 2011;258(1):254-260.

38. Wasser MN, Geelkerken RH, Kouwenhoven M, et al. Systolically gated 3D phase contrast MRA of mesenteric arteries in suspected mesenteric ischemia. J Comput Assist Tomogr 1996;20(2):262-268.

39. Waaler BA, Eriksen M, Toska K. The effect of meal size on postprandial increase in cardiac output. Acta Physiol Scand 1991;142(1):33-39.

40. Poole JW, Sammartano RJ, Boley SJ. Hemodynamic basis of the pain of chronic mesenteric ischemia. Am J Surg 1987;153(2):171-176.

Tables:

Table 1: Average Preprandial Volumetric Flow Rates (mL/min/kg)

	Control	CMI-	CMI+
SCAo	48.2 ± 17.6	44.6 ± 15.6	36.5 ± 10.4
IRAo	15.5 ± 7.81	16.5 ± 6.50	19.1 ± 3.88
LRA	5.00 ± 3.40	6.40 ± 2.73	6.68 ± 8.44
RRA	4.85 ± 2.42	6.18 ± 2.99	6.01 ± 6.37
SMA	5.97 ± 3.15	8.04 ± 4.35	7.59 ± 3.13
CA	11.8 ± 7.88	**6.72 ± 3.54**	7.80 ± 3.51
SMV	6.61 ± 2.66	6.89 ± 4.14	**10.7 ± 3.64**
SV	6.52 ± 4.18	6.46 ± 3.63	5.21 ± 1.89
PV	14.1 ± 5.57	13.5 ± 4.40	17.7 ± 5.71

Volumetric flow rates are expressed as mean ± 1 standard deviation. **Bold** indicates statistical significance ($p < 0.05$) compared to controls. Underline indicates statistical significance ($p < 0.05$) between CMI+ and CMI- groups. SCAo = supraceliac aorta, IRAo = infrarenal aorta, LRA = left renal artery, RRA = right renal artery, SMA = superior mesenteric artery, CA = celiac artery, SMV = superior mesenteric vein, SV = splenic vein, and PV = portal vein.

Table 2: Average Postprandial Volumetric Flow Rates (mL/min/kg)

	Control	CMI-	CMI+
SCAo	55.3 ± 19.9	54.2 ± 22.3	**35.3 ± 11.3**
IRAo	14.0 ± 6.15	19.3 ± 6.93	18.6 ± 7.00
LRA	4.94 ± 2.91	6.33 ± 2.74	6.37 ± 9.29
RRA	5.21 ± 2.72	6.33 ± 3.70	3.82 ± 4.18
SMA	11.1 ± 5.00	12.5 ± 6.40	9.37 ± 4.52
CA	11.0 ± 7.00	7.00 ± 4.42	8.17 ± 3.96
SMV	14.2 ± 4.56	16.7 ± 7.23	15.5 ± 8.60
SV	5.80 ± 2.52	5.94 ± 3.85	4.46 ± 1.67
PV	20.6 ± 5.91	23.1 ± 6.56	20.8 ± 10.3

Volumetric flow rates are expressed as mean ± 1 standard deviation. **Bold** indicates statistical significance ($p < 0.05$) compared to controls. Underline indicates statistical significance ($p < 0.05$) between CMI+ and CMI- groups. SCAo = supraceliac aorta, IRAo = infrarenal aorta, LRA = left renal artery, RRA = right renal artery, SMA = superior mesenteric artery, CA = celiac artery, SMV = superior mesenteric vein, SV = splenic vein, and PV = portal vein.

Table 3: Average Percent Change in Flow (%)

	Control *(# Vessels visualized out of 20)*	**CMI-** *(# Vessels visualized out of 13)*	**CMI+** *(# Vessels Visualized out of 6)*
SCAo	15.7 ± 14.8 *(20)*	21.1 ± 16.6 *(13)*	**-2.57 ± 12.1** *(5)*
IRAo	-7.03 ± 24.4 *(18)*	13.0 ± 31.1 *(12)*	-3.16 ± 27.1 *(5)*
LRA	3.58 ± 15.4 *(19)*	2.03 ± 21.0 *(13)*	-19.9 ± 26.1 *(6)*
RRA	6.97 ± 17.5 *(20)*	-0.95 ± 19.0 *(11)*	-35.7 ± 37.1 *(5)*
SMA	98.8 ± 80.7 *(20)*	62.7 ± 66.5 *(13)*	**23.5 ± 32.7** *(6)*
CA	-3.73 ± 18.9 *(19)*	0.93 ± 35.6 *(12)*	4.52 ± 8.53 *(6)*
SMV	132 ± 80.7 *(19)*	178 ± 147 *(13)*	**40.3 ± 55.6** *(6)*
SV	-4.76 ± 32.3 *(17)*	-3.77 ± 36.0 *(13)*	-11.7 ± 19.4 *(6)*
PV	56.7 ± 47.9 *(19)*	72.1 ± 50.4 *(13)*	**11.7 ± 30.9** *(6)*

Percentages are expressed as mean ± 1 standard deviation. **Bold** indicates statistical significance ($p < 0.05$) compared to controls. Underline indicates statistical significance ($p < 0.05$) between CMI+ and CMI- groups. SCAo = supraceliac aorta, IRAo = infrarenal aorta, LRA = left renal artery, RRA = right renal artery, SMA = superior mesenteric artery, CA = celiac artery, SMV = superior mesenteric vein, SV = splenic vein, and PV = portal vein.

Figure Legends:

Figure 1: Phase contrast (PC) angiograms of the mesenteric vasculature created from 4D flow MRI complex difference data. Anterior (a) and posterior (b) views of the segmented angiogram for a healthy (61-year-old, male) control subject. Note the high vascular detail. "Trimmed" PC angiogram from the same subject, including only relevant venous (blue) and arterial (red) vasculature needed for quantitative analysis (c).

Figure 2: (a) Velocity color-coded pathlines soon after systole in the arterial vasculature of a healthy (61-year-old, male) control subject. (b) Velocity color-coded streamline images in the venous system soon after systole for the same control subject. 2D cut-planes (a,b) are shown for all mesenteric vessels being quantitatively analyzed. Inset image shows time-resolved, manual segmentation of the CA in a customized software package.

*Figure 3: Average percent changes in blood flow for each subgroup. * indicates statistical significance ($p<0.05$).*

Figure 4: Correlation analysis of venous and arterial flow measurements. (Left) Difference in blood flow between SCAo and IRAo measurements ($\overline{Q}_{loss}$) plotted against the sum of flow from all branching arteries between the measured SCAo and IRAo segments ($\overline{Q}_{branch}$). The dotted gray line represents true conservation of flow (i.e. one-to-one correlation). (Right) Portal vein flow measurements ($\overline{Q}_{PV}$) plotted against the sum of flow from the splenic and superior mesenteric veins ($\overline{Q}_{SV} + \overline{Q}_{SMV}$).

Figure 5: (a) CA compression from median arcuate ligament syndrome with collateral compensation from SMA in a fasting 29-year-old female. Flow from the SMA is redirected through the pancreaticoduodenal arcade to supply the splenic and left gastric branches of the CA. In the PC angiogram, the CA cannot be visualized due to flow obstruction in this vessel. (b) SMA occlusion and celiac narrowing in a fasting 42-year-old male with CMI. Numerous collaterals from the IMA, via the Arc of Riolan, and CA, via the pancreaticoduodenal arcades, supply blood to the SMA. The proximal SMA cannot be visualized on the PC angiogram due to absence of flow. Note that the IMA was included in the field of view in this patient and can be seen at the bottom of the figure. Image inset shows an abnormality in the aorta (situated superoposterior to the celiac root), likely a developing atherosclerotic lesion.

Figures:

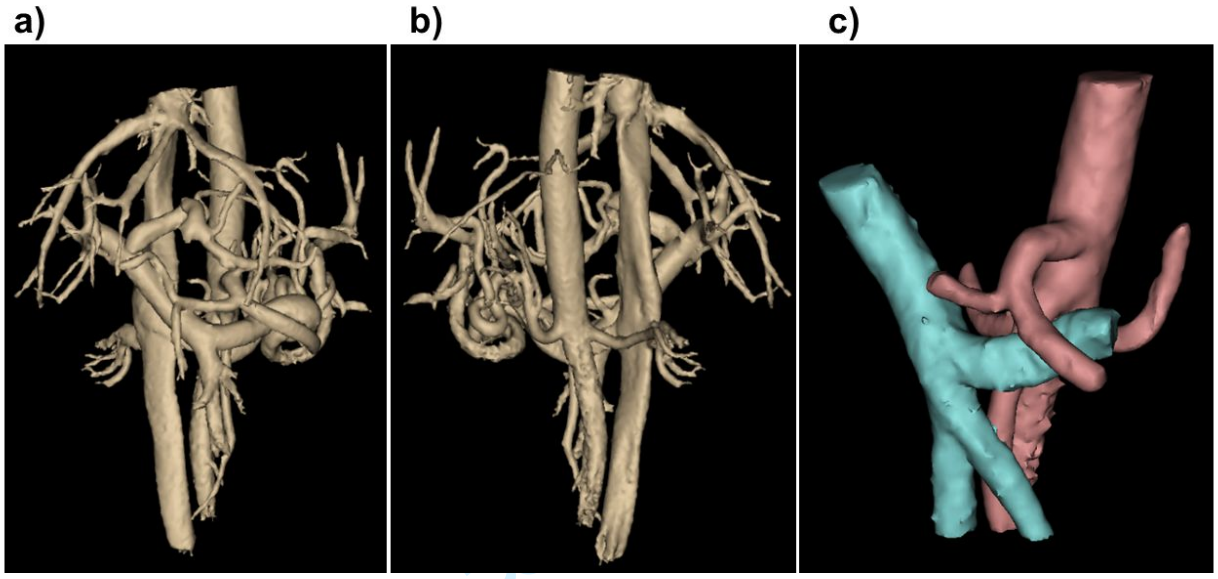

Figure 1: Phase contrast (PC) angiograms of the mesenteric vasculature created from 4D flow MRI complex difference data. Anterior (a) and posterior (b) views of the segmented angiogram for a healthy (61-year-old, male) control subject. Note the high vascular detail. "Trimmed" PC angiogram from the same subject, including only relevant venous (blue) and arterial (red) vasculature needed for quantitative analysis (c).

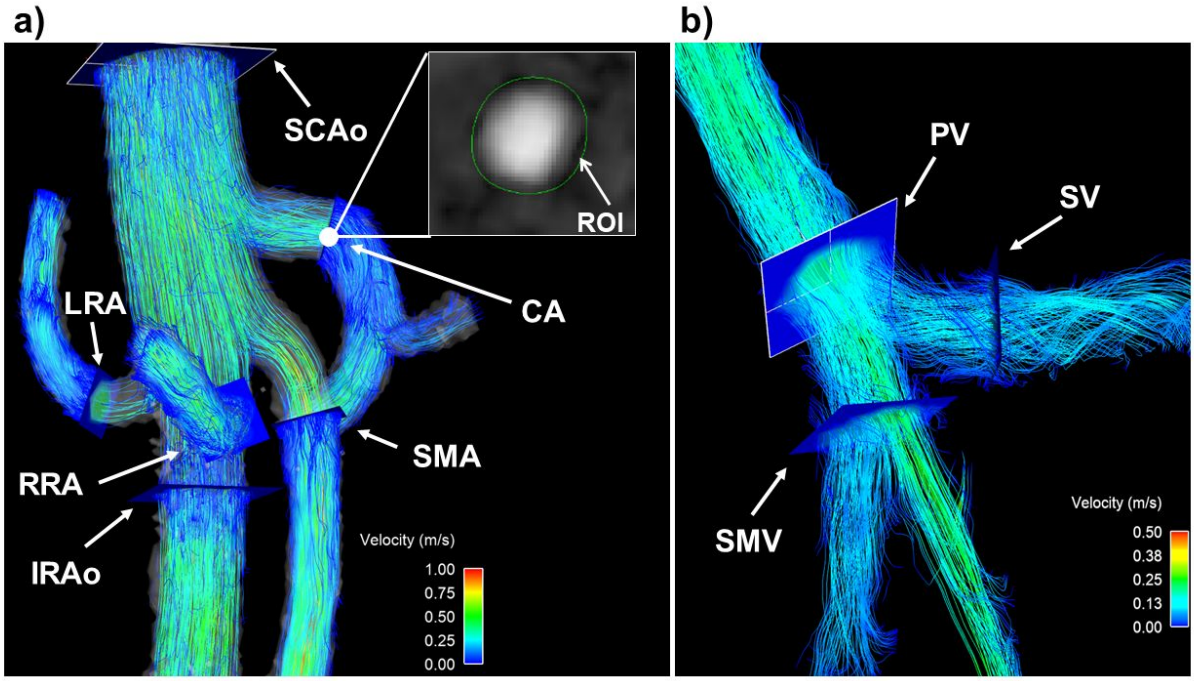

Figure 2: (a) Velocity color-coded pathlines soon after systole in the arterial vasculature of a healthy (61-year-old, male) control subject. (b) Velocity color-coded streamline images in the venous system soon after systole for the same control subject. 2D cut-planes (a,b) are shown for all mesenteric vessels being quantitatively analyzed. Inset image shows time-resolved, manual segmentation of the CA in a customized software package.

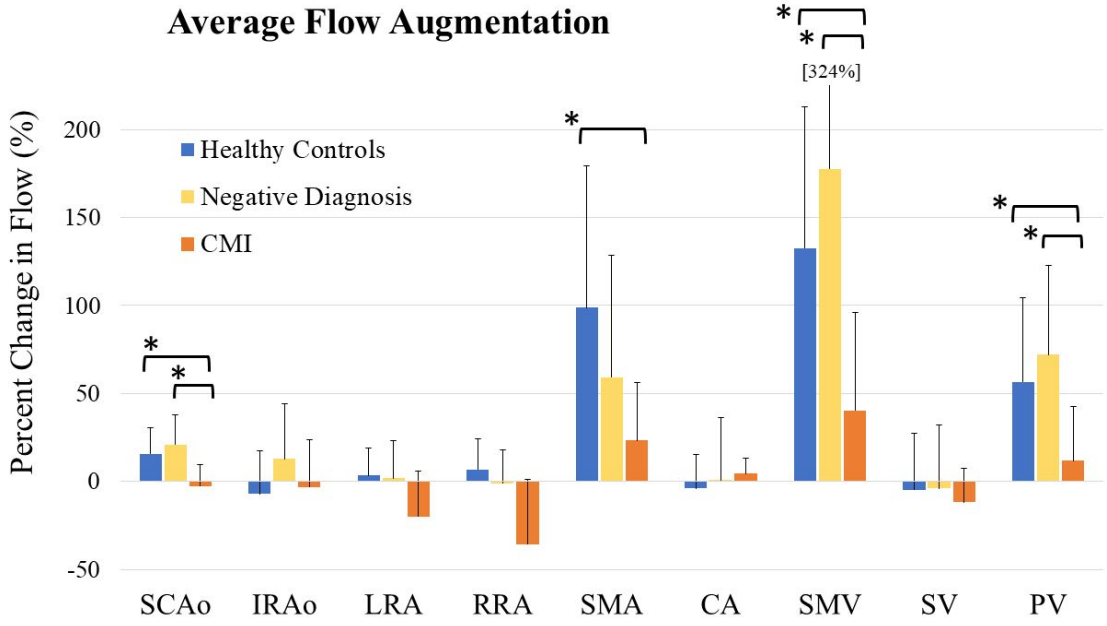

*Figure 3: Average percent changes in blood flow for each subgroup. * indicates statistical significance ($p<0.05$).*

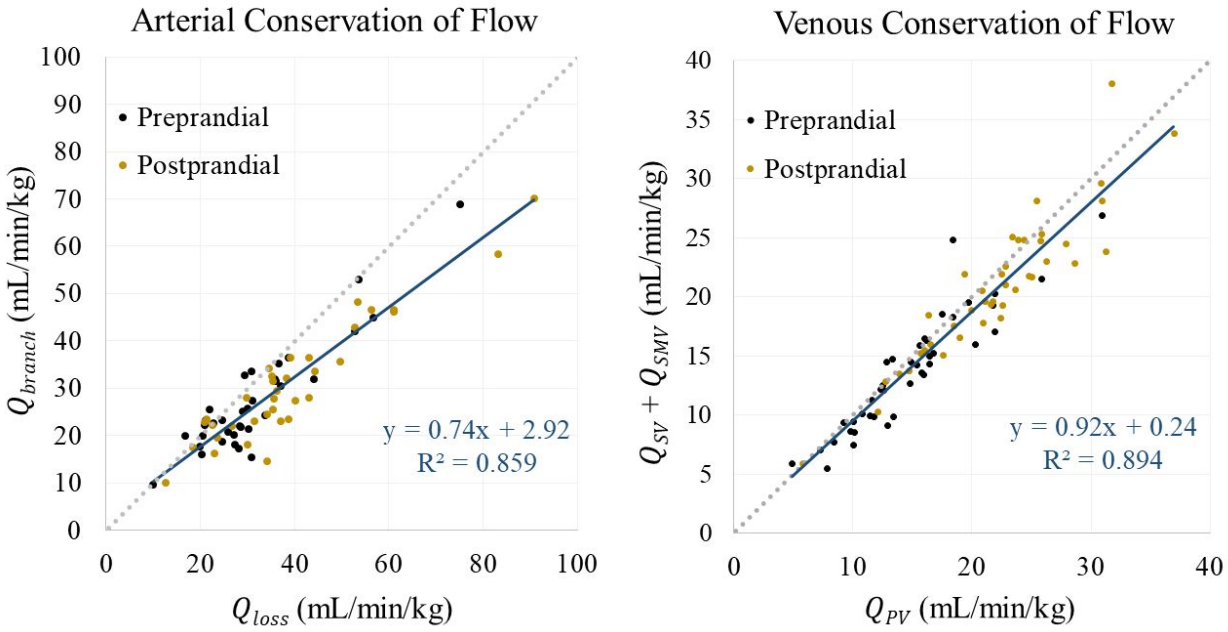

Figure 4: Correlation analysis of venous and arterial flow measurements. (Left) Difference in blood flow between SCAo and IRAo measurements ($\overline{Q}_{loss}$) plotted against the sum of flow from all branching arteries between the measured SCAo and IRAo segments ($\overline{Q}_{branch}$). The dotted gray line represents true conservation of flow (i.e. one-to-one correlation). (Right) Portal vein flow measurements ($\overline{Q}_{PV}$) plotted against the sum of flow from the splenic and superior mesenteric veins ($\overline{Q}_{SV} + \overline{Q}_{SMV}$).

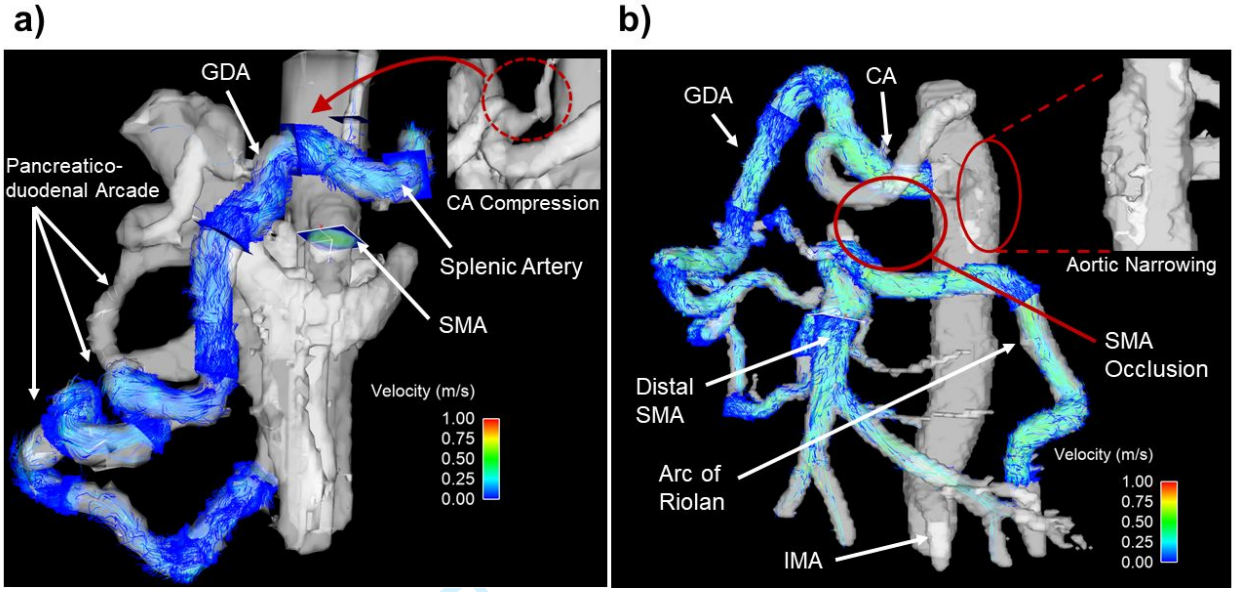

Figure 5: (a) CA compression from median arcuate ligament syndrome with collateral compensation from SMA in a fasting 29-year-old female. Flow from the SMA is redirected through the pancreaticoduodenal arcade to supply the splenic and left gastric branches of the CA. In the PC angiogram, the CA cannot be visualized due to flow obstruction in this vessel. (b) SMA occlusion and celiac narrowing in a fasting 42-year-old male with CMI. Numerous collaterals from the IMA, via the Arc of Riolan, and CA, via the pancreaticoduodenal arcades, supply blood to the SMA. The proximal SMA cannot be visualized on the PC angiogram due to absence of flow. Note that the IMA was included in the field of view in this patient and can be seen at the bottom of the figure. Image inset shows an abnormality in the aorta (situated superoposterior to the celiac root), likely a developing atherosclerotic lesion.

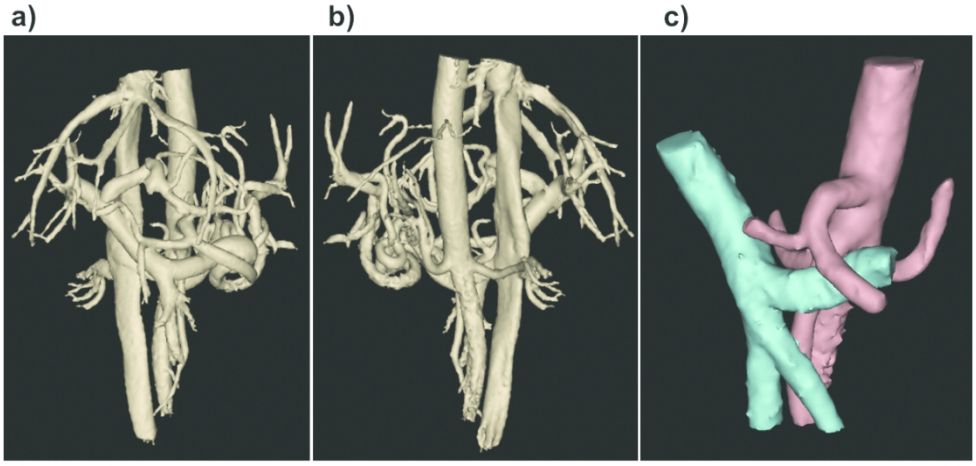

Phase contrast (PC) angiograms of the mesenteric vasculature created from 4D flow MRI complex difference data. Anterior (a) and posterior (b) views of the segmented angiogram for a healthy (61-year-old, male) control subject. Note the high vascular detail. "Trimmed" PC angiogram from the same subject, including only relevant venous (blue) and arterial (red) vasculature needed for quantitative analysis (c).

338x190mm (96 x 96 DPI)

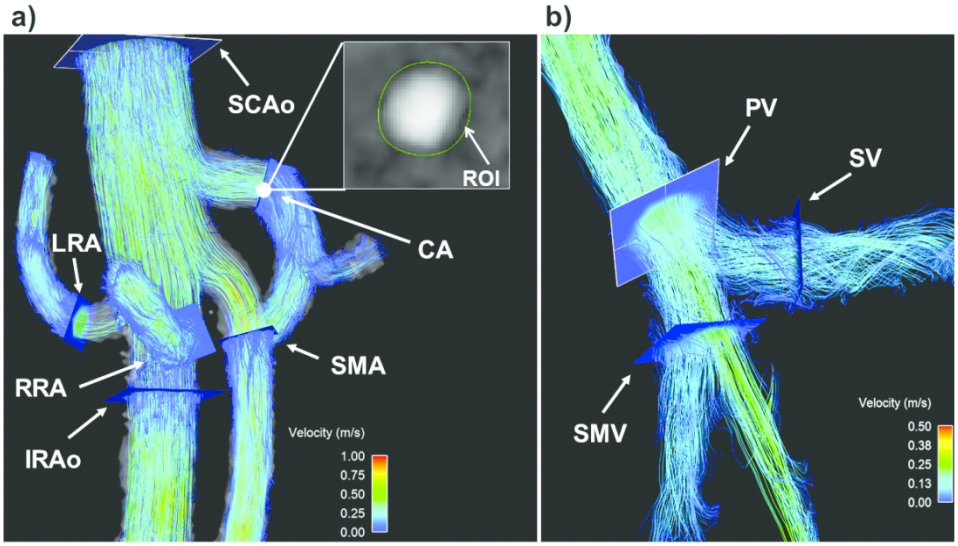

(a) Velocity color-coded pathlines soon after systole in the arterial vasculature of a healthy (61-year-old, male) control subject. (b) Velocity color-coded streamline images in the venous system soon after systole for the same control subject. 2D cut-planes (a,b) are shown for all mesenteric vessels being quantitatively analyzed. Inset image shows time-resolved, manual segmentation of the CA in a customized software package.

338x190mm (96 x 96 DPI)

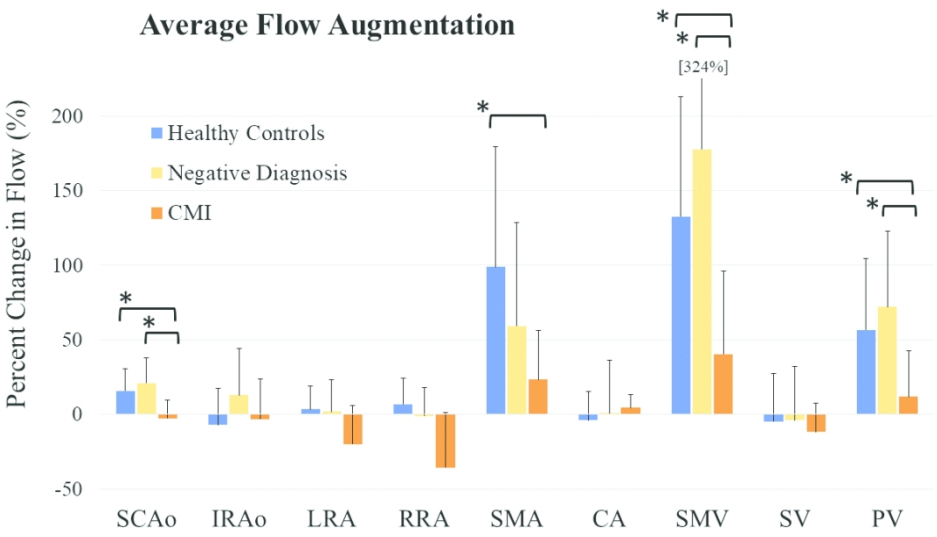

Average percent changes in blood flow for each subgroup. * indicates statistical significance ($p<0.05$).

338x190mm (96 x 96 DPI)

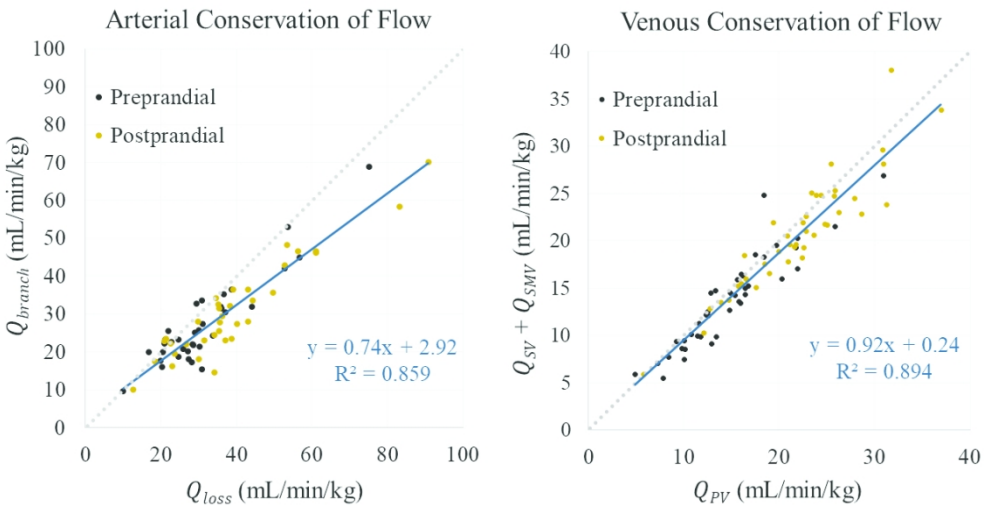

Correlation analysis of venous and arterial flow measurements. (Left) Difference in blood flow between SCAo and IRAo measurements (Q_{loss}) plotted against the sum of flow from all branching arteries between the measured SCAo and IRAo segments (Q_{branch}). The dotted gray line represents true conservation of flow (i.e. one-to-one correlation). (Right) Portal vein flow measurements (Q_{PV}) plotted against the sum of flow from the splenic and superior mesenteric veins (Q_{SV}+Q_{SMV}).

338x190mm (96 x 96 DPI)

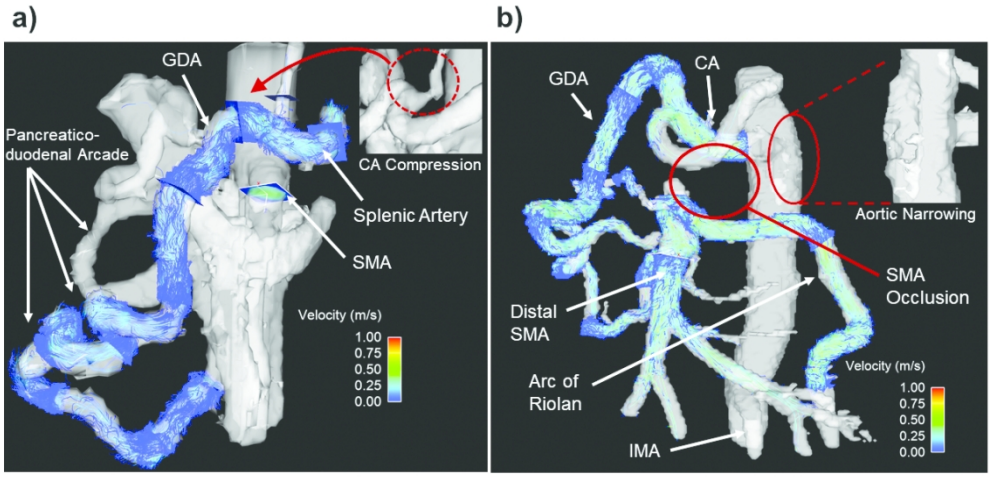

(a) CA compression from median arcuate ligament syndrome with collateral compensation from SMA in a fasting 29-year-old female. Flow from the SMA is redirected through the pancreaticoduodenal arcade to supply the splenic and left gastric branches of the CA. In the PC angiogram, the CA cannot be visualized due to flow obstruction in this vessel. (b) SMA occlusion and celiac narrowing in a fasting 42-year-old male with CMI. Numerous collaterals from the IMA, via the Arc of Riolan, and CA, via the pancreaticoduodenal arcades, supply blood to the SMA. The proximal SMA cannot be visualized on the PC angiogram due to absence of flow. Note that the IMA was included in the field of view in this patient and can be seen at the bottom of the figure. Image inset shows an abnormality in the aorta (situated superoposterior to the celiac root), likely a developing atherosclerotic lesion.

338x190mm (96 x 96 DPI)

Table 1: Average Preprandial Volumetric Flow Rates (mL/min/kg)

	Control	CMI-	CMI+
SCAo	48.2 ± 17.6	44.6 ± 15.6	36.5 ± 10.4
IRAo	15.5 ± 7.81	16.5 ± 6.50	19.1 ± 3.88
LRA	5.00 ± 3.40	6.40 ± 2.73	6.68 ± 8.44
RRA	4.85 ± 2.42	6.18 ± 2.99	6.01 ± 6.37
SMA	5.97 ± 3.15	8.04 ± 4.35	7.59 ± 3.13
CA	11.8 ± 7.88	**6.72 ± 3.54**	7.80 ± 3.51
SMV	6.61 ± 2.66	6.89 ± 4.14	**10.7 ± 3.64**
SV	6.52 ± 4.18	6.46 ± 3.63	5.21 ± 1.89
PV	14.1 ± 5.57	13.5 ± 4.40	17.7 ± 5.71

Volumetric flow rates are expressed as mean ± 1 standard deviation. **Bold** indicates statistical significance ($p < 0.05$) compared to controls. Underline indicates statistical significance ($p < 0.05$) between CMI+ and CMI- groups. SCAo = supraceliac aorta, IRAo = infrarenal aorta, LRA = left renal artery, RRA = right renal artery, SMA = superior mesenteric artery, CA = celiac artery, SMV = superior mesenteric vein, SV = splenic vein, and PV = portal vein.

152x127mm (96 x 96 DPI)

Table 2: Average Postprandial Volumetric Flow Rates (mL/min/kg)

	Control	CMI-	CMI+
SCAo	55.3 ± 19.9	54.2 ± 22.3	**35.3 ± 11.3**
IRAo	14.0 ± 6.15	19.3 ± 6.93	18.6 ± 7.00
LRA	4.94 ± 2.91	6.33 ± 2.74	6.37 ± 9.29
RRA	5.21 ± 2.72	6.33 ± 3.70	3.82 ± 4.18
SMA	11.1 ± 5.00	12.5 ± 6.40	9.37 ± 4.52
CA	11.0 ± 7.00	7.00 ± 4.42	8.17 ± 3.96
SMV	14.2 ± 4.56	16.7 ± 7.23	15.5 ± 8.60
SV	5.80 ± 2.52	5.94 ± 3.85	4.46 ± 1.67
PV	20.6 ± 5.91	23.1 ± 6.56	20.8 ± 10.3

Volumetric flow rates are expressed as mean ± 1 standard deviation. **Bold** indicates statistical significance ($p < 0.05$) compared to controls. Underline indicates statistical significance ($p < 0.05$) between CMI+ and CMI- groups. SCAo = supraceliac aorta, IRAo = infrarenal aorta, LRA = left renal artery, RRA = right renal artery, SMA = superior mesenteric artery, CA = celiac artery, SMV = superior mesenteric vein, SV = splenic vein, and PV = portal vein.

152x127mm (96 x 96 DPI)

Table 3: Average Percent Change in Flow (%)

	Control *(# Vessels visualized out of 20)*	CMI- *(# Vessels visualized out of 13)*	CMI+ *(# Vessels Visualized out of 6)*
SCAo	15.7 ± 14.8 *(20)*	21.1 ± 16.6 *(13)*	**-2.57 ± 12.1** *(5)*
IRAo	-7.03 ± 24.4 *(18)*	13.0 ± 31.1 *(12)*	-3.16 ± 27.1 *(5)*
LRA	3.58 ± 15.4 *(19)*	2.03 ± 21.0 *(13)*	-19.9 ± 26.1 *(6)*
RRA	6.97 ± 17.5 *(20)*	-0.95 ± 19.0 *(11)*	-35.7 ± 37.1 *(5)*
SMA	98.8 ± 80.7 *(20)*	62.7 ± 66.5 *(13)*	**23.5 ± 32.7** *(6)*
CA	-3.73 ± 18.9 *(19)*	0.93 ± 35.6 *(12)*	4.52 ± 8.53 *(6)*
SMV	132 ± 80.7 *(19)*	178 ± 147 *(13)*	**40.3 ± 55.6** *(6)*
SV	-4.76 ± 32.3 *(17)*	-3.77 ± 36.0 *(13)*	-11.7 ± 19.4 *(6)*
PV	56.7 ± 47.9 *(19)*	72.1 ± 50.4 *(13)*	**11.7 ± 30.9** *(6)*

Percentages are expressed as mean ± 1 standard deviation. **Bold** indicates statistical significance ($p < 0.05$) compared to controls. Underline indicates statistical significance ($p < 0.05$) between CMI+ and CMI- groups. SCAo = supraceliac aorta, IRAo = infrarenal aorta, LRA = left renal artery, RRA = right renal artery, SMA = superior mesenteric artery, CA = celiac artery, SMV = superior mesenteric vein, SV = splenic vein, and PV = portal vein.

139x127mm (96 x 96 DPI)